Accurate Determination of Radiation Patterns from Near-Field Measurements in Highly Reflective Environments

Josef Knapp[1], Thomas F. Eibert[1],
[1]Chair of High-Frequency Engineering, of Electrical and Computer Engineering,
Technical University of Munich, Munich, Germany, josef.knapp@tum.de

***Abstract*—The radiation pattern of an antenna under test is determined from measurements in a highly reflective, fully metallic measurement environment similar to a reverberation chamber. The undesired influence of the reflecting walls is eliminated by processing the data obtained for a large number of frequencies and different probe locations in the chamber. The post-processing concept effectively combines temporal and spatial filtering of the measured signals in an innovative field synthesis concept. S-Band measurements show the effectiveness of the proposed processing concepts. The accuracy is comparable to anechoic measurements, however, for the cost of increased measurement and post-processing effort.**

***Index Terms*—antenna measurement, near-field far-field transformation, echo suppression.**

I. Introduction

Measurements of the radiation pattern of an antenna under test (AUT) are conventionally performed in anechoic environments, where high effort is put into suppressing any undesired echo signal, which may corrupt the measurements. If one is interested in the performance of an AUT under extreme environmental conditions, such as very high or very low temperatures or very low pressures, it is not possible to equip the chamber with absorbing materials. Instead the measurements have to be performed in fully metallic, so called thermo vacuum chambers, which have similar electrical properties as reverberation chambers without a mode stirrer. In such a measurement environment, the received signal is disturbed by massive echo contributions, which have to be accounted for in the data post-processing. Since the available space inside a thermo vacuum chamber is very limited, measurements can only be obtained in near-field (NF) distance to the AUT. The far-field (FF) radiation pattern of these NF measurements can be calculated with a suitable near-field far-field transformation (NFFFT) only if the echo perturbations can be removed from the measured signals, either prior to the transformation, or within the transformations, or afterwards.

Since echo perturbations are a major error source in NF antenna measurements [1], echo suppression techniques have been of great research interest and a variety of methods for the treatment of echoic measurements exist. The available techniques can be roughly categorized into two groups, namely time domain and frequency domain techniques.

Time gating techniques [2], [3], [4] utilize the fact that the traveling times are different for the direct line of sight (LOS) paths and any reflected path. The number of necessary frequency points is determined by the shortest path length differences which should be separable and the signal decay time inside the chamber [5]. The path length resolution determines the necessary bandwidth and the unambiguous time span is determined by the frequency step between the samples. Frequency domain techniques [6], [7], [8] utilize information about the location and size of the AUT to separate signals, which may have its origin inside the AUT volume, from signals, which must originate from a different location.

Neither of the two techniques alone will be able to remove the echo perturbations completely. The frequency domain methods can not remove echo contributions from echo currents, which are present inside the AUT volume due to multiple interactions between the AUT and the scatterers. The time domain techniques reach their limitation if either the necessary bandwidth for the desired path length resolution exceeds the usable bandwidth of the AUT or if the LOS signal has not decayed before the first reflected signals reach the probe.

There have been attempts for obtaining the radiation pattern from measurements in a reverberation chamber [9], [10], however, the obtained accuracies are far from the accuracies one would obtain in anechoic measurement sites.

Therefore, in this work a natural combination of time domain and frequency domain techniques is presented. The signal of a virtual probe array is synthesized and it is shown that a smart choice of the array weights results in an effective combination of time gating and spatial filtering echo suppression methods.

In order to show the effectiveness of the proposed methods, measurements have been obtained in a fully metallic chamber, which has been built especially for testing the capabilities of echo suppression techniques in a worst case environment.

II. Field Synthesis for Virtual Probe Arrays

The signals received by a probe at different locations and different frequencies can be combined in order to synthesize the behavior of a virtual array with a desired receiving characteristic, which is insensitive for the echo signals.

A linear combination of frequency domain data corresponds to multiplying the corresponding time domain data with a

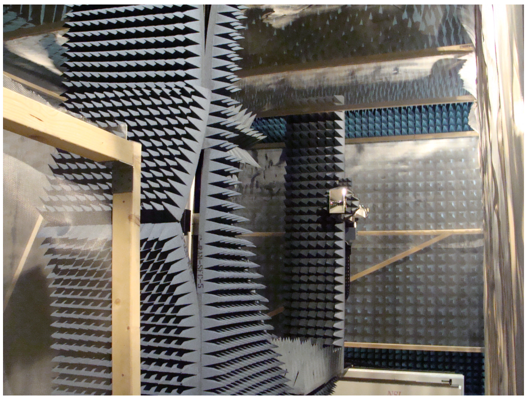

Fig. 1. Picture of the DRH18 probe mounted on the probe tower inside the Mosquito chamber. Only moving parts have been equipped by absorbers. The AUT positioner is in the foreground.

Fig. 2. Picture of the DRH400 used as AUT.

suitable gating window. This time gating can be very efficiently performed utilizing the Fast Fourier Transform (FFT) and inverse Fast Fourier Transform (IFFT). After time gating the measurements at all probe locations, one is usually only interested in the signal at a particular frequency ω_0, reducing the effort for finding convenient array coefficients at a single frequency only.

The received signal $S_{21,\mathrm{array}}$ of a N-element virtual array is given by

$$S_{21,\mathrm{array}} = \sum_{i=1}^{N} \alpha_i \, S_{21,i} \, , \tag{1}$$

where $\alpha_i \in \mathbb{C}$ are the coefficients of the linear combination and $S_{21,i}$ is the received signal of the probe at the ith probe position, respectively.

The field $\boldsymbol{E}_{\mathrm{array}}$, radiated by the virtual array, is given by

$$\boldsymbol{E}_{\mathrm{array}}(\boldsymbol{r}) = \sum_{i=1}^{N} \alpha_i \, \boldsymbol{E}_i(\boldsymbol{r}) \, , \tag{2}$$

where $\boldsymbol{E}_i(\boldsymbol{r})$ is the radiated field from the probe at the ith location. By choosing the α_i in order to minimize the field at the scatterer locations, the probe is effectively made immune against the echo perturbations as the echo contribution in the signal is negligible in this case as the probe only illuminates the AUT and not the scatterers.

III. RESULTS

For the evaluation of the effectiveness of the approach, measurements have been performed in a fully metallic measurement environment, which has been built into the anechoic chamber at the Technical University of Munich (TUM). The realized measurement chamber has dimensions 7.5 m × 4 m × 3.5 m and the walls consist of a metallic aluminum net. The utilized probe is a DRH18 dual ridged horn, which can be seen in Fig. 1 mounted on the probe tower, which can be moved along the x-, y-, and z- direction. The considered AUT is a DRH400 dual ridged horn, which can be seen in Fig. 2. The AUT has been mounted on the AUT positioner, shown in the foreground of Fig. 1. The AUT positioner can be rotated around its ϑ- and φ-axis, respectively, such that full spherical measurements are possible. Measurements have been obtained for 132 different probe positions located in four planes with distances $z_1 = 2.664\,\mathrm{m}$, $z_2 = 2.704\,\mathrm{m}$, $z_3 = 2.784\,\mathrm{m}$ and $z_4 = 2.904\,\mathrm{m}$ to the AUT. For each probe position, a full spherical measurement has been obtained by rotating the AUT around its two axes with a 2.5° sampling step. All measurements have been obtained for 1001 frequencies from 1.5 GHz to 3.5 GHz with a frequency step of 2 MHz. The frequency requirements have been deduced from a preliminary measurement of the AUT in the chamber from which the decay time of the fields inside the chamber has been estimated.

In a first processing step, the NF data has been time gated with a time gate dependent on the distance between the probe and the AUT. The time gated data at 2.5 GHz has been further processed and combined to form a virtual array as described in the previous section. The coefficients α_i have been determined in a field synthesis step solving a minimization problem in order to focus the array fields towards the AUT and minimizing the magnitude of the array field near the reflective walls. The data from the virtual array has then been processed with the Fast Irregular Antenna Field Transformation Algorithm (FIAFTA) [11], [12], as if the data would have been obtained with the array in the first place, taking the full receiving characteristic of the virtual array into account for probe correction. The retrieved FFs can be seen in Figs. 3 and 4.

The gray solid line denotes the FF obtained by FIAFTA from the uncorrected NF measurements. The blue solid line denotes the FF after the NF data has been cleaned by time gating and spatial filtering and thereafter further processed by FIAFTA. The orange dashed line denotes the reference, which has been obtained from NF measurements in the anechoic chamber (without the metallic nets inside the chamber). The reference FF has again been computed via FIAFTA from the unperturbed

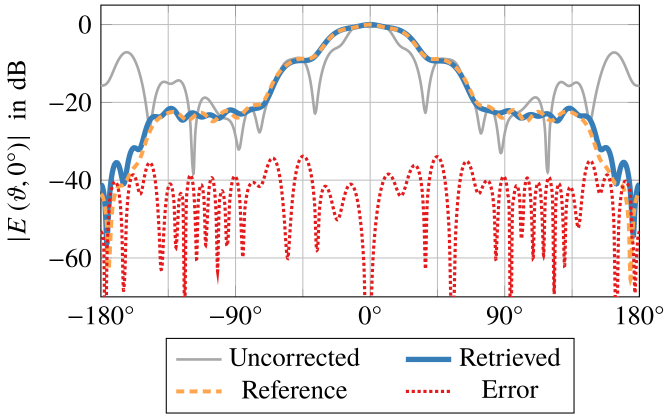

Fig. 3. Retrieved co-polar component of the FF in the cut at $\varphi = 90°$.

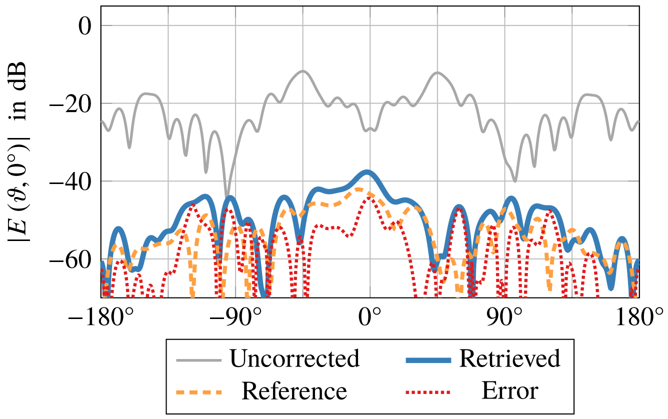

Fig. 4. Retrieved cross-polar component of the FF in the cut at $\varphi = 90°$.

measurements in the anechoic chamber. All retrieved FFs have been normalized to their maximum values, respectively. The dotted red line denotes the error ϵ between the retrieved FF and the reference FF, computed by

$$\epsilon = 20 \log\left(\left|\frac{E}{E_{\max}} - \frac{E_{\text{ref}}}{E_{\text{ref,max}}}\right|\right) . \tag{3}$$

Figure 3 shows the retrieved FFs co-polarized component along the cut at $\varphi = 90°$ and Fig. 4 shows the corresponding cross-polar component. The maximum error in the co-polar component is about −34 dB, while the error is below −40 dB for most directions. The maximum cross-polar error is below −42 dB and the mean square error

$$\epsilon_{\text{RMSE}} = \sqrt{\oint \left|\frac{E}{E_{\max}} - \frac{E_{\text{ref}}}{E_{\text{ref,max}}}\right|^2 \mathrm{d}\Omega}, \tag{4}$$

computed from integrating the squared error over the whole sphere, is $\epsilon_{\text{RMSE}} = 0.00030$.

IV. Conclusion

A general echo suppression method has been presented as a linear combination of all available measurements at a fixed AUT position. Sufficiently many samples, both in frequency and spatial domain have been utilized to get rid of the undesired echo contributions within the measurement signal. While the combination of different probe signals in frequency domain corresponds to well known time gating techniques, the combination of the spatial domain data effectively results in generating a virtual probe array, which is not sensitive for the fields generated by scatterers outside the AUT volume. Applying the echo suppression methods on real measurement data obtained in a fully metal cage environment has shown, that accuracies can be obtained, which are similar to those known from fully anechoic measurements.

Acknowledgment

This work was carried out under the Technology Research Programme of, and funded by, the European Space Agency. The view expressed in this publication can in no way be taken to reflect the opinion of the European Space Agency.

The authors are grateful to Laurent Trougnou and Maurice Paquay from the European Space Agency for their support in this project.

References

[1] A. C. Newell, “Error analysis techniques for planar near-field measurements,” *IEEE Transactions on Antennas and Propagation*, vol. 36, no. 6, pp. 754–768, 1988.

[2] M. D. Blech, M. M. Leibfritz, R. Hellinger, D. Geier, F. A. Maier, A. M. Pietsch, and T. F. Eibert, “A time domain spherical near-field measurement facility for UWB antennas employing a hardware gating technique,” *Advances in Radio Science*, vol. 8, pp. 243–250, 2010.

[3] B. N. Levitas and D. M. Ponomarev, “Antenna measurements in time domain,” in *Antennas and Propagation Society International Symposium*, vol. 1, Jul. 1996, pp. 573–576.

[4] T. K. Sarkar and O. Pereira, “Using the matrix pencil method to estimate the parameters of a sum of complex exponentials,” *Antennas and Propagation Magazine, IEEE*, vol. 37, no. 1, pp. 48–55, 1995.

[5] M. M. Leibfritz, M. D. Blech, F. M. Landstorfer, and T. F. Eibert, “A comparison of software-and hardware-gating techniques applied to near-field antenna measurements,” *Advances in Radio Science*, vol. 5, pp. 43–48, 2007.

[6] S. Loredo, M. R. Pino, F. Las-Heras, and T. K. Sarkar, “Echo identification and cancellation techniques for antenna measurement in non-anechoic test sites,” *IEEE Antennas and Propagation Magazine*, vol. 46, no. 1, pp. 100–107, 2004.

[7] S. F. Gregson, A. C. Newell, G. E. Hindman, and M. J. Carey, “Application of mathematical absorber reflection suppression to planar near-field antenna measurements,” in *Proceedings of the 5th European Conference on Antennas and Propagation (EUCAP)*. IEEE, 2011, pp. 3412–3416.

[8] J. L. A. Quijano, L. Scialacqua, J. Zackrisson, L. J. Foged, M. Sabbadini, and G. Vecchi, “Suppression of undesired radiated fields based on equivalent currents reconstruction from measured data,” *IEEE Antennas and Wireless Propagation Letters*, vol. 10, pp. 314–317, 2011.

[9] M. Á. Garca-Fernndez, D. Carsenat, and C. Decroze, “Antenna radiation pattern measurements in reverberation chamber using plane wave decomposition,” *IEEE Transactions on Antennas and Propagation*, vol. 61, no. 10, pp. 5000–5007, Oct. 2013.

[10] Q. Xu, Y. Huang, L. Xing, C. Song, Z. Tian, S. S. Aljaafreh, and M. Stanley, “3D antenna radiation pattern reconstruction in a reverberation chamber using spherical wave decomposition,” *IEEE Transactions on Antennas and Propagation*, vol. 65, no. 4, pp. 1728–1739, Apr. 2017.

[11] C. H. Schmidt, M. M. Leibfritz, and T. F. Eibert, “Fully probe-corrected near-field far-field transformation employing plane wave expansion and diagonal translation operators,” *IEEE Transactions on Antennas and Propagation*, vol. 56, no. 3, pp. 737–746, 2008.

[12] T. F. Eibert and C. H. Schmidt, “Multilevel fast multipole accelerated inverse equivalent current method employing RaoWiltonGlisson discretization of electric and magnetic surface currents,” *IEEE Transactions on Antennas and Propagation*, vol. 57, no. 4, pp. 1178–1185, 2009.